Atomic Data and Nuclear Data Tables 148 (2022) 101534

Contents lists available at ScienceDirect

Atomic Data and Nuclear Data Tables

journal homepage: www.elsevier.com/locate/adt

Complete collision data set for electrons scattering on molecular hydrogen and its isotopologues: III. Vibrational excitation via electronic excitation and radiative decay

Liam H. Scarlett [a,*], Daniel K. Boyle [a], Mark C. Zammit [b], Yuri Ralchenko [c], Igor Bray [a], Dmitry V. Fursa [a]

[a] Curtin Institute for Computation and Department of Physics and Astronomy, Curtin University, Perth, Western Australia 6102, Australia
[b] Theoretical Division, Los Alamos National Laboratory, Los Alamos, NM 87545, USA
[c] National Institute of Standards and Technology, Gaithersburg, MD 20899-8422, USA

ARTICLE INFO

Article history:
Received 18 May 2022
Received in revised form 15 July 2022
Accepted 15 July 2022
Available online 10 August 2022

Dataset link: https://mccc-db.org

ABSTRACT

We present state-resolved cross sections for vibrational excitation via electronic excitation followed by radiative decay (ERD), for electrons scattering on all bound vibrational levels of the ground electronic state ($X\ ^1\Sigma_g^+$) of molecular hydrogen and its isotopologues (H_2, HD, HT, D_2, DT and T_2). We consider excitation of the singlet $n = 2$–3 states (where n refers to the united-atoms-limit principle quantum number) and account for all possible decay pathways back to the bound vibrational levels of the ground electronic state ($X\ ^1\Sigma_g^+$) to produce an estimate for the ERD cross sections. A selection of the results are presented in graphical form and a full data set is provided as both numerical values and analytic fit functions in supplementary data files. The uncertainty in the cross sections is estimated to be 11%, except for scattering on the highest bound vibrational level of HD, HT, D_2, and DT, where the uncertainty is 21%. The data can be downloaded from the MCCC database at mccc-db.org.

* Corresponding author.
E-mail address: liam.scarlett@curtin.edu.au (L.H. Scarlett).

https://doi.org/10.1016/j.adt.2022.101534
0092-640X/

Contents

1. Introduction

Above the electronic inelastic threshold, vibrational excitation of H_2 and its isotopologues occurs predominantly via electronic excitation followed by radiative decay back to the ground electronic state. This process is commonly referred to as excitation-radiative-decay (ERD), or alternatively the E–V process. The primary importance of ERD is as a mechanism for the production of vibrationally-excited molecules, which can play a major role in determining the properties of many industrial and astrophysical plasmas (see Ref. [1] for further discussion).

In the previous papers in this series [2,3], we have presented a complete set of vibrationally-resolved cross sections for excitation of the $n=2$–3 electronic states of H_2 and its five isotopologues from the ground electronic state (n here refers to the united-atoms-limit principle quantum number). These calculations were performed using the *ab-initio* molecular convergent close-coupling (MCCC) method, with the adiabatic-nuclei approximation applied to the treatment of nuclear motion [4,5]. Here we apply these cross sections in the evaluation of ERD cross sections for electrons scattering on the vibrationally-excited ground state of H_2, D_2, T_2, HD, HT, and DT, for incident energies from threshold to 500 eV.

The first calculations of ERD cross sections for H_2 were performed by Hiskes [6], who identified the initial excitation of the $B\ ^1\Sigma_u^+$ and $C\ ^1\Pi_u$ states as the most important contributions to the process. Later, ERD calculations for H_2 and D_2 were performed using the semi-classical impact-parameter method (IP) considering initial excitation of the $B\ ^1\Sigma_u^+$ and $C\ ^1\Pi_u$ states by Celiberto et al. [7], and the $B'\ ^1\Sigma_u^+$ and $D\ ^1\Pi_u$ states by Laricchiuta et al. [8]. More recent MCCC calculations [1] of the ERD cross sections for H_2 explicitly considered the contributions from excitation of the $B\ ^1\Sigma_u^+$, $C\ ^1\Pi_u$, $EF\ ^1\Sigma_g^+$, $B'\ ^1\Sigma_u^+$, and $D\ ^1\Pi_u$ states, and approximated the ERD contribution from higher singlet states. These results were found to be up to a factor of two lower than the IP calculations at low to intermediate incident energies. In the present work, the MCCC ERD calculations for scattering on H_2 are improved, and extended to consider the isotopologues. These cross sections will be useful for modeling low-collision-rate plasmas, where radiative decay is the dominant de-excitation mechanism. For plasmas where the collision rates are comparable to the radiative decay rates, more sophisticated modeling which accounts for collisions with excited electronic states is required [9]. Atomic units are used throughout this work, unless otherwise specified.

2. Theory

Within the non-relativistic approximation, radiative decays must conserve the target spin, and hence the study of decays to the singlet ground state of H_2 only requires consideration of excitations into the singlet system. We label the states involved in the ERD process according to the following schematic:

$$\underbrace{iv_i \longrightarrow fv_f}_{\text{impact excitation}} \boxed{\text{radiative decays}} \longrightarrow iv_i', \tag{1}$$

where v_i is the initial vibrational level in the ground electronic state (denoted i), f and v_f are the target electronic and vibrational states following the initial electron-impact excitation, and v_i' is the vibrational level back in the ground state following a sequence of radiative decays.

The probability of radiative decay from state fv_f to state iv_i', accounting for all possible decay pathways, is denoted P_{iv_i',fv_f}. The ERD cross section is then given by

$$\sigma^{\mathrm{ERD}}_{iv_i',f,iv_i} = \sum_{v_f} P_{iv_i',fv_f}(1 - F^{\mathrm{PD}}_{fv_f,iv_i})\sigma_{fv_f,iv_i}, \tag{2}$$

where σ_{fv_f,iv_i} is the $iv_i \to fv_f$ excitation cross section, and $F^{\mathrm{PD}}_{fv_f,iv_i}$ is the fraction of the excitation cross section which leads to predissociation (obtained from Ref. [10]). The total ERD cross section for a given initial state iv_i is found by summing Eq. (2) over the excited electronic states f:

$$\sigma^{\mathrm{ERD}}_{iv_i} = \sum_f \sigma^{\mathrm{ERD}}_{f,iv_i}. \tag{3}$$

In the present work the sum over electronic states includes all $n=2$–3 singlet states (where n is the united-atoms-limit principle quantum number). The vibrationally-resolved excitation cross sections for each of these states were presented in the previous papers in this series [2,3].

Transition probabilities were calculated as outlined by Glass-Maujean [11]. The probability of radiative decay from a bound vibrational level v of an electronic state p to the bound level v' in electronic state p' is given by

$$A_{p'v',pv} = GC(\varepsilon_{p'v'} - \varepsilon_{pv})^3 \left|\langle \nu_{p'v'}|D_{p',p}(R)|\nu_{pv}\rangle\right|^2, \tag{4}$$

where G is a degeneracy factor determined by the electronic transition, $C = 2.141 \times 10^{10}$ sec^{-1}, $D_{p',p}$ is the electronic dipole moment curve between the two states, and $\nu_{pv}(R)$ are bound vibrational wave functions with energies ε_{pv}. We have utilized the dipole moment curves compiled by Fantz and Wünderlich [12] from various sources in the literature [13–17]. The method for obtaining ν_{pv} and a summary of the number of levels in each electronic state was given in Refs. [2,3]. We note that Fantz and Wünderlich [12] also calculated the vibrationally-resolved radiative-decay probabilities for the states considered here, but aside for transitions to the $b\ ^3\Sigma_u^+$ state they do not consider transitions into the dissociative continuum which we require to properly normalize the probabilities.

The probability for transitions into the vibrational continuum of the electronic state p' is given by

$$\frac{dA_{p',pv}}{d\epsilon} = GC(\varepsilon_{p'v'} - \varepsilon_{pv})^3 \left|\langle v_{p'\epsilon}|D_{p',p}(R)|v_{pv}\rangle\right|^2, \quad (5)$$

where $v_{p'\epsilon}$ is a suitably-normalized dissociative vibrational wave function with energy ϵ. The correct choice of vibrational-wave normalization was discussed previously in Ref. [18]. Normalized transition probabilities (or branching ratios) are obtained by dividing Eqs. (4)–(5) by

$$N_{pv} = \sum_{p'v'} A_{p'v',pv} + \sum_{p'} \int \frac{dA_{p',pv}}{d\epsilon} d\epsilon, \quad (6)$$

where the sum/integration is over all states with energy below ε_{pv}. The total $fv_f \rightarrow iv_i'$ transition probabilities P_{iv_i',fv_f} were evaluated using a recursive algorithm which accounts for all possible decay pathways through an arbitrary number of intermediate states.

3. Cross sections and analytic fits

We have performed ERD calculations firstly considering the contributions from initial excitation of the $B\ ^1\Sigma_u^+$, $C\ ^1\Pi_u$ $B'\ ^1\Sigma_u^+$ and $D\ ^1\Pi_u$ states, to allow comparison with the IP calculations Celiberto et al. [19], Laricchiuta et al. [8], and secondly considering the contributions from all $n = 2$ and 3 singlet states. The uncertainty associated with neglecting the $n > 3$ states is discussed in Section 4. In Fig. 1 we present a comparison with the IP calculations of the $v_i = 0 \rightarrow v_i' = 0$ and $v_i = 0 \rightarrow v_i' = 5$ ERD cross sections for H_2. In the high-energy limit, the IP results converge to the MCCC cross sections (when the same sets of intermediate electronic states are used), while in the low- to intermediate-energy range the IP calculations overestimate the cross section. Since the IP method is semiclassical in nature, it is expected to be accurate only in the high-energy limit. By contrast, the MCCC method is expected to be accurate to within about 10% across the entire energy range. The MCCC calculations including the contribution from all $n = 2$–3 singlet are between 5 and 15% larger than those considering only the $B\ ^1\Sigma_u^+$, $C\ ^1\Pi_u$, $B'\ ^1\Sigma_u^+$, and $D\ ^1\Pi_u$ states. Further examples of the MCCC ERD cross sections for a number of different initial vibrational levels of H_2 are given in Graph 1.

In Fig. 2 the ERD cross sections for the $v_i = 0 \rightarrow v_i' = 0$ transition for H_2 and its isotopologues are compared. The cross section is largest for H_2, and decreases with increasing nuclear reduced mass. Further illustrations of the isotopic effect are presented in Fig. 3. In the top panel, the ERD cross section for 60 eV electrons incident on the $v_i = 0$ level of each isotopologue is presented as a function of the final vibrational level (v_i') energy. While the heavier isotopologues have a smaller cross section for ERD ending in a given vibrational level, they also have a larger number of bound vibrational levels. The combined effect of these two facts is shown in the bottom panel of Fig. 3, where the $v_i = 0$ ERD cross section is summed over final vibrational levels v_i'. Here, there is only a small difference between the cross sections for the different isotopologues.

Cross sections have been calculated for all possible ERD $v_i \rightarrow v_i'$ transitions in each isotopologue, and are available in text files as outlined in Section 5. In addition to numerical cross sections, we also provide analytic fits for each transition, employing the following analytic fit function:

$$\sigma(x) = \frac{x-1}{x} \cdot \left(\frac{a_0^2}{x}\ln x + \frac{a_1}{x} + \frac{a_2}{x^2} + \frac{a_3}{x^3} + \frac{a_4}{x^4} + \frac{a_5}{x^5}\right). \quad (7)$$

Here, $x = E_{\rm in}/E_0$, where E_0 is the threshold energy. For the ERD process the threshold energy is equivalent to the threshold for

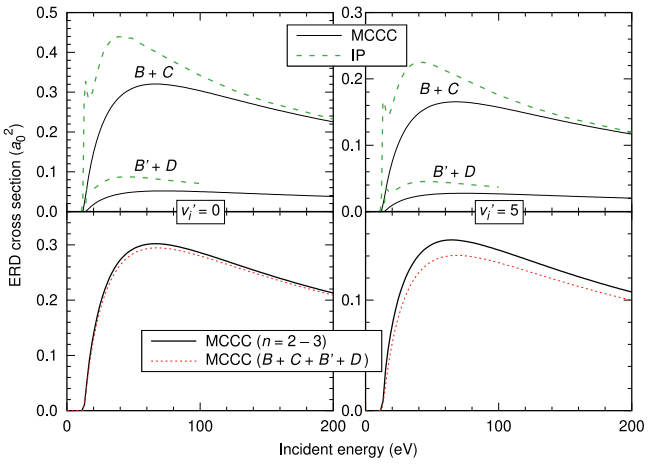

Fig. 1. Excitation radiative decay (ERD) cross sections for electrons scattering on the $X\ ^1\Sigma_g^+(v_i = 0)$ level of H_2, leading to radiative decays to the $v_i' = 0$ (left) and $v_i' = 5$ (right) vibrational levels of the $X\ ^1\Sigma_g^+$ state. In the top row, the MCCC calculations including contributions from the $B\ ^1\Sigma_u^+$ and $C\ ^1\Pi_u$ states are compared with the impact-parameter (IP) calculations of Celiberto et al. [19], and contributions from the $B'\ ^1\Sigma_u^+$ and $D\ ^1\Pi_u$ states are compared with the IP calculations of Laricchiuta et al. [8]. In the bottom row, the MCCC calculations including all four of these states are compared with the MCCC results considering all $n = 2$–3 excitations.

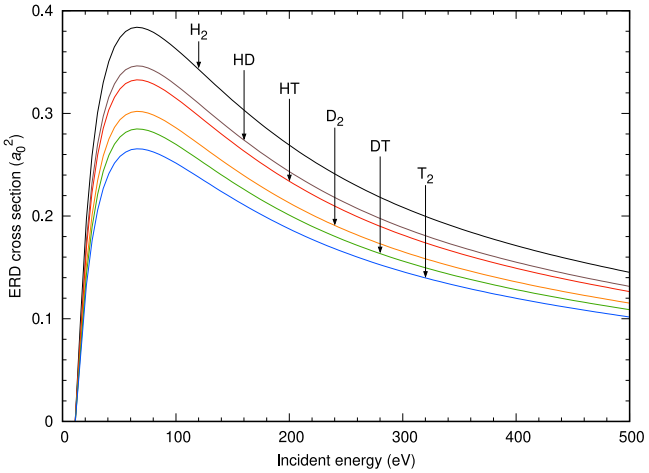

Fig. 2. Isotope effect in the $v_i = 0 \rightarrow v_i' = 0$ excitation radiative decay (ERD) cross sections.

excitation of the $B\ ^1\Sigma_u^+(v = 0)$ state. The fitting parameters are also provided in text files as outlined in Section 5.

Calculations of the ERD process can also be used to produce cross sections for molecular dissociation via radiative decay into the $X\ ^1\Sigma_g^+$ state vibrational continuum. Such studies have been performed for H_2 and D_2 in the IP calculations [8,19], and for H_2 in the previous MCCC calculations [1]. In the present work we do not consider this process, instead deferring dissociation studies for the isotopologues of H_2 for a more detailed treatment including all important dissociation pathways as was done for H_2 in Refs. [20,21].

4. Uncertainty estimates

The two sources of uncertainty in the ERD calculations are the uncertainty in the underlying MCCC excitation cross sections, and the error introduced by neglecting the contributions from initial excitations to $n > 3$ states. Previously [2,3], we estimated

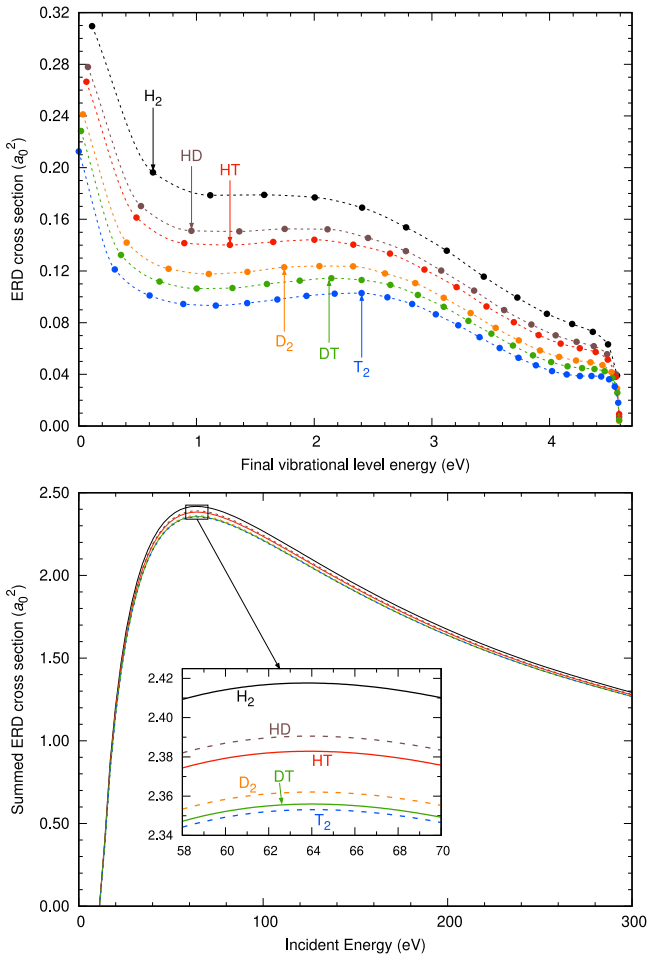

Fig. 3. Excitation radiative decay (ERD) cross sections for electrons scattering on the $v_i = 0$ level of H_2 and its isotopologues. Top panel: Cross sections at 60 eV incident energy presented as a function of the final vibrational level energy (relative to the $X\ ^1\Sigma_g^+$ equilibrium energy). Bottom panel: ERD cross sections summed over final vibrational level presented as a function of incident energy.

the uncertainty in the MCCC cross sections to be 10%, except for scattering on the HD($v = 17$), HT($v = 18$), D_2($v = 21$), and DT($v = 23$) levels, for which the uncertainty is up to 20% due to the less accurate target structure at the larger internuclear separations spanned by those states. In order to provide an upper bound on the error due to neglecting the $n > 3$ excitations, Fig. 4 compares the total bound singlet excitation cross section from the MCCC(210) model with the sum of the $n = 2$–3 singlet excitation cross sections for scattering on the $v_i = 0$–14 levels of H_2 at 60 eV. The discrepancy between the two is roughly 5% for large v_i, and less than 5% for smaller v_i. We hence liberally apply an additional 5% uncertainty to the ERD calculations, resulting in a total uncertainty estimate of $\sqrt{10^2 + 5^2} \approx 11\%$. For scattering on the HD($v = 17$), HT($v = 18$), D_2($v = 21$), and DT($v = 23$) levels, the total uncertainty is 21%.

5. Accessing the data

The ERD cross sections are provided in supplementary data files named in the format

```
MCCC-el-[mol]-X1Sg_vf=[vf].ERD.X1Sg_vi=[vi].txt
```

where `[mol]` is the molecule name (`H2`, `HD`, `HT`, `D2`, `DT`, or `T2`), `[vf]` is the final vibrational level (v_i'), and `[vi]` is the initial

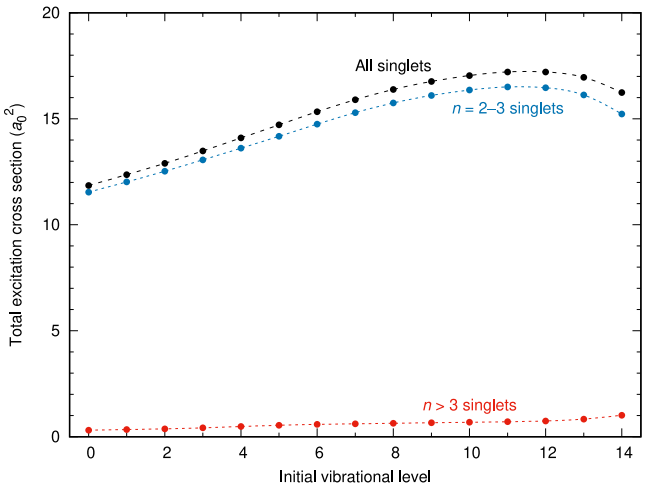

Fig. 4. Sum of 60 eV excitation cross sections as a function of initial vibrational level for all singlet states of H_2 in the MCCC(210) model, compared to the sum of the $n - 2$–3 singlet excitation cross sections. The difference between the two indicates the upper bound on the error introduced in the ERD calculations by neglecting the $n > 3$ excitations.

vibrational level (v_i). The fitting parameters are provided in files named in the format

```
MCCC-el-[mol]-X1Sg.ERD.X1Sg_vi=[vi]_fit.txt
```

with each file containing parameters for transitions to all v_i' from a given v_i. The format of the cross section and fitting parameter files is identical to the examples given in Ref. [2]. The present data and all other MCCC calculations can also be downloaded from the MCCC database at mccc-db.org.

6. Conclusions

We have presented a complete set of excitation-radiative-decay (ERD) cross sections for electrons scattering on the vibrationally-excited ground state of H_2, HD, HT, D_2, DT and T_2. Analytic fits have been provided for all transitions, and the uncertainties in the cross sections have been estimated. For scattering on H_2 and D_2, the present calculations represent a substantial improvement in accuracy over the previously available data, while for the remaining isotopologues the present results are, to our knowledge, the first such data presented.

Declaration of competing interest

The authors declare that they have no known competing financial interests or personal relationships that could have appeared to influence the work reported in this paper.

Data availability

The MCCC cross sections are available in the supplementary material, and the MCCC database at https://mccc-db.org.

Acknowledgments

We are grateful to U. Fantz, and D. Wünderlich for supplying their data in electronic form. This work was supported by the United States Air Force Office of Scientific Research and The Australian Research Council. HPC resources were provided by the Pawsey Supercomputing Centre with funding from the Australian Government and Government of Western Australia, and the Texas

Advanced Computing Center (TACC) at The University of Texas at Austin. M.C.Z. would like to specifically acknowledge the support of the Los Alamos National Laboratory (LANL) Laboratory Directed Research and Development program Project No. 20200356ER. LANL is operated by Triad National Security, LLC, for the National Nuclear Security Administration of the U.S. Department of Energy under Contract No. 89233218NCA000001.

Appendix A. Supplementary data

Supplementary material related to this article can be found online at https://doi.org/10.1016/j.adt.2022.101534.

References

[1] L.H. Scarlett, J.K. Tapley, J.S. Savage, D.V. Fursa, M.C. Zammit, I. Bray, Plasma Sources Sci. Technol. 28 (2019a) 025004.
[2] L.H. Scarlett, D.V. Fursa, M.C. Zammit, I. Bray, Yu. Ralchenko, K.D. Davie, At. Data Nucl. Data Tables 137 (2021a) 101361.
[3] L.H. Scarlett, D.V. Fursa, M.C. Zammit, I. Bray, Yu. Ralchenko, At. Data Nucl. Data Tables 139 (2021b) 101403.
[4] M.C. Zammit, D.V. Fursa, J.S. Savage, I. Bray, J. Phys. B At. Mol. Opt. Phys. 50 (2017) 123001.
[5] L.H. Scarlett, J.S. Savage, D.V. Fursa, I. Bray, M.C. Zammit, Eur. Phys. J. D 74 (2020) 36.
[6] J.R. Hiskes, J. Appl. Phys. 70 (1991) 3409.
[7] R. Celiberto, M. Capitelli, M. Capitelli, A. Laricchiuta, Phys. Scr. T 96 (2002) 32.
[8] A. Laricchiuta, R. Celiberto, F. Esposito, M. Capitelli, Plasma Sources Sci. Technol. 15 (2006) 10.
[9] G. Colonna, L.D. Pietanza, G. D'Ammando, R. Celiberto, M. Capitelli, A. Laricchiuta, Eur. Phys. J. D 71 (2017) 279.
[10] X. Liu, P.V. Johnson, C.P. Malone, J.A. Young, D.E. Shemansky, I. Kanik, J. Phys. B At. Mol. Opt. Phys. 42 (2009) 185203.
[11] M. Glass-Maujean, At. Data Nucl. Data Tables 30 (1984) 301.
[12] D. Fantz, U. Wünderlich, Atom. Data Nucl. Data Tables 92 (2006) 853.
[13] G. Wolniewicz, L. Staszewska, J. Mol. Spectrosc. 220 (2003a) 45.
[14] L. Dressler, K. Wolniewicz, Ber. Bunsenges. Phys. Chem. 99 (1995) 246.
[15] G. Wolniewicz, L. Staszewska, J. Mol. Spectrosc. 217 (2003b) 181.
[16] L. Dressler, K. Wolniewicz, Canadian J. Phys. 62 (1984) 1706.
[17] L. Wolniewicz, J. Mol. Spectrosc. 180 (1996) 398.
[18] L.H. Scarlett, D.V. Fursa, J. Knol, M.C. Zammit, I. Bray, Phys. Rev. A 103 (2021c) L020801.
[19] R. Celiberto, U.T. Lamanna, M. Capitelli, Phys. Rev. A 50 (1994) 4778.
[20] L.H. Scarlett, J.K. Tapley, D.V. Fursa, M.C. Zammit, J.S. Savage, I. Bray, Eur. Phys. J. D 72 (2018) 34.
[21] L.H. Scarlett, J.S. Savage, D.V. Fursa, M.C. Zammit, I. Bray, Atoms 7 (2019b) 75.

Explanation of Graphs

Graph 1. **Excitation radiative decay cross sections for electron collisions with $H_2(X\ ^1\Sigma_g^+)$.**
Each panel represents a different initial vibrational level in the $X\ ^1\Sigma_g^+$ state, while each line represents a different final vibrational level in the $X\ ^1\Sigma_g^+$ after electronic excitation and subsequent radiative decay.

v_i Initial vibrational level in the $X\ ^1\Sigma_g^+$ state
v_i' Final vibrational level in the $X\ ^1\Sigma_g^+$ state

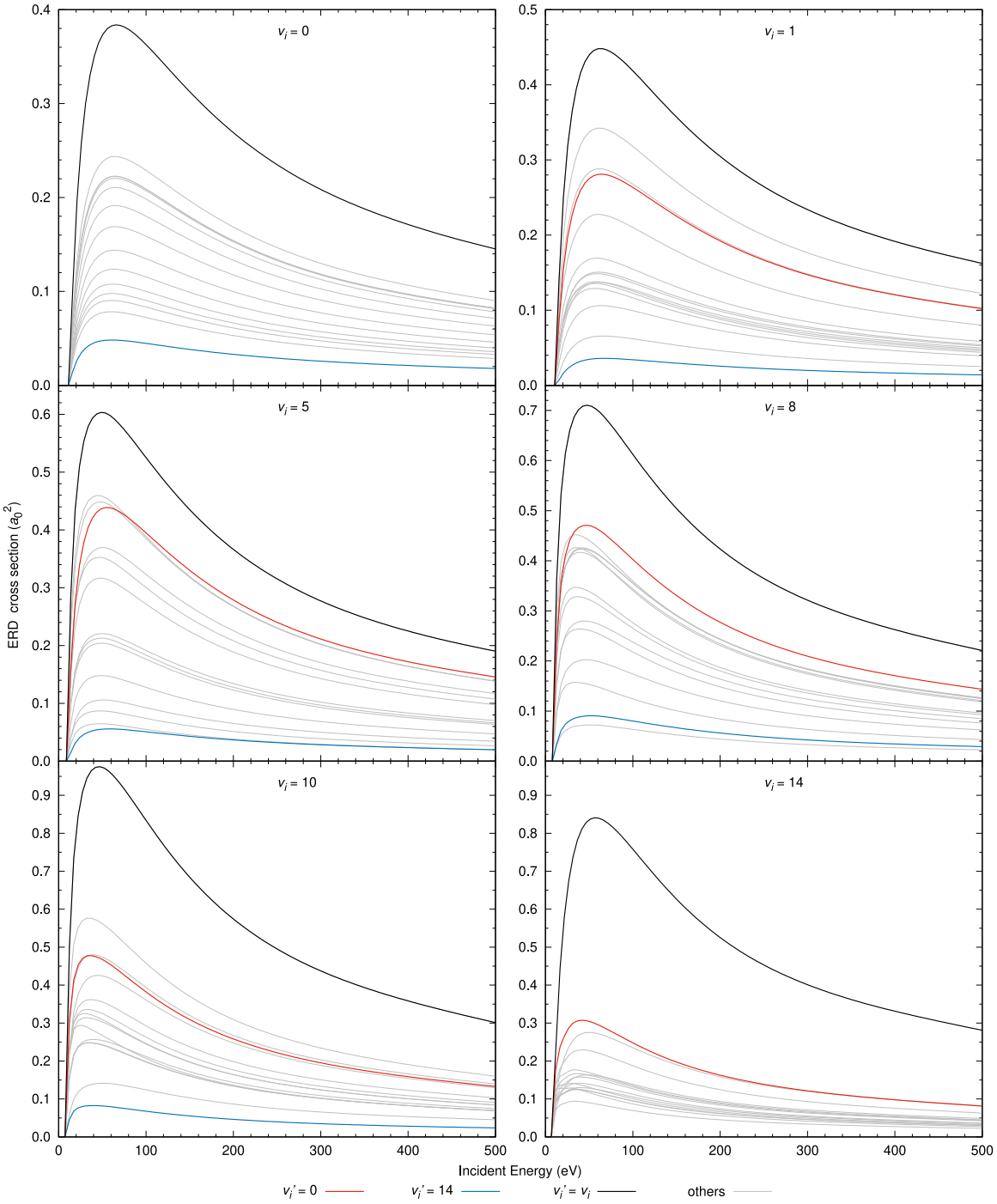

Graph 1. Excitation radiative decay (ERD) cross sections for electron collisions with $H_2(X\ ^1\Sigma_g^+)$. See explanation of graphs.